Spin connection and boundary states in a topological insulator

V. Parente,[1,*] P. Lucignano,[1,2] P. Vitale,[1,3] A. Tagliacozzo,[1,2] and F. Guinea[4]

[1]*Dipartimento Scienze Fisiche, Università di Napoli Federico II, Via Cintia, I-80126 Napoli, Italy*

[2]*CNR-SPIN, Monte S. Angelo-Via Cintia, I-80126, Napoli, Italy*

[3]*INFN, Via Cintia, I-80126, Napoli, Italy*

[4]*Instituto de Ciencia de Materiales de Madrid (CSIC), Sor Juana Inés de la Cruz 3, E-28049 Madrid, Spain*

(Received 2 November 2010; revised manuscript received 14 January 2011; published 22 February 2011)

We study the surface resistivity of a three-dimensional topological insulator when the boundaries exhibit a nontrivial curvature. We obtain an analytical solution for a spherical topological insulator, and we show that a nontrivial quantum spin connection emerges from the three-dimensional band structure. We analyze the effect of the spin connection on the scattering by a bump on a flat surface. Quantum effects induced by the geometry lead to resonances when the electron wavelength is comparable to the size of the bump.

DOI: 10.1103/PhysRevB.83.075424 PACS number(s): 73.20.−r, 73.23.−b, 72.10.Fk

I. INTRODUCTION

Strong topological insulators (TIs) are a new class of materials with a bulk gap but surface states defined on surfaces of all orientations,[1–4] making the boundaries gapless. The number of surface states at a flat surface with a given orientation is odd, and each of them shows a conical singularity, described by the two-dimensional Dirac equation.[4] Localized states also exist at other lattice defects, such as screw dislocations.[5–7]

The transport features of electrons at the surfaces of TIs is being intensively studied. The wave functions have an internal spinorial structure made up of two slowly varying components related by time reversal invariance. Backscattering, due to smooth perturbations that preserve the time reversal symmetry, is forbidden, making the transport properties of these compounds similar to those of graphene in the absence of intervalley scattering.[8] Surfaces with a finite curvature allow for scattering processes due to the existence of a nontrivial metric, which has been studied in the classical limit,[9] when wave packets are well approximated by point particles following classical trajectories.

An analysis of the electronic properties of curved surfaces of TIs requires information about the way in which a nontrivial metric changes the effective Dirac equation. It is well known that the Dirac equation can be written on a curved space time introducing the spin connection and the rotation of Dirac matrices.[10] The existence of the spin connection has been postulated in topological insulators.[11] The emergence of the spin connection from the combination of the three-dimensional electronic structure of a TI and the two-dimensional metric of a boundary with intrinsic curvature has not been studied so far.

In the next section, we analyze the surface states for the simplest curved boundary with a nontrivial metric, the sphere. The conservation of the angular momentum in this geometry allows us to calculate the entire spectrum of surface states and to show that the spin connection term is induced in the effective surface Hamiltonian. We use this information in Sec. III to analyze the effect of the curvature in the scattering by a bump in a flat surface, a process considered in the classical limit in Ref. 9. Related processes can be defined in graphene with topological defects.[12] Technical details of the calculations are discussed in the appendixes, including an analytical study in Appendix A of the boundary states in a cylinder, calculated numerically in Ref. 13. The boundary of a cylinder can be considered a surface without intrinsic curvature and spin connection.

II. TOPOLOGICAL INSULATOR WITH A SPHERICAL BOUNDARY

The surface states of model single-particle Hamiltonians for a TI have been studied particularly for a flat boundary[14] and for an infinite cylinder boundary surface.[13] A minimal model reproducing the band structure of a TI requires four orbitals, related in pairs by time reversal symmetry.[15] A further simplification includes just the contributions linear in momentum that appear in the Hamiltonian in Ref. 15:

$$\mathcal{H} = \hat{\gamma}^0 \Delta + \hbar v_F \hat{\gamma}^i k_i, \tag{1}$$

where v_F is the Fermi velocity and the matrices $\hat{\gamma}^a$ are given in terms of Pauli matrices by $\hat{\gamma}^0 = \mathbb{I}_{2\times 2} \otimes \tau_z$, $\hat{\gamma}^1 = \sigma_x \otimes \tau_x$, $\hat{\gamma}^2 = -\sigma_y \otimes \tau_x$, and $\hat{\gamma}^3 = \sigma_z \otimes \tau_x$. Here $\mathbb{I}_{2\times 2}$ is the 2×2 identity, while σ_a and τ_b denote matrices in the spin and even-odd orbital parity spaces, respectively. This Hamiltonian satisfies time reversal symmetry $T = \mathcal{K}\, i\sigma_y \otimes \mathbb{I}_{2\times 2}$ ($\mathcal{K}$ is the complex conjugation). Bulk eigenfunctions in Cartesian coordinates are

$$|\Psi_{1,\pm}\rangle = \frac{1}{N_\pm} \begin{pmatrix} \epsilon_\pm(\vec{\mathbf{k}}) + \Delta \\ \hbar v_F k_z \\ 0 \\ \hbar v_F k_- \end{pmatrix} e^{i\vec{k}\cdot\vec{r}},$$
$$|\Psi_{2,\pm}\rangle = \frac{1}{N_\pm} \begin{pmatrix} 0 \\ \hbar v_F k_+ \\ \epsilon_\pm(\vec{\mathbf{k}}) + \Delta \\ -\hbar v_F k_z \end{pmatrix} e^{i\vec{k}\cdot\vec{r}} \tag{2}$$

($k_\pm = k_x \pm i k_y$), where the band energies are $\epsilon_\pm(\vec{\mathbf{k}}) \equiv \pm\sqrt{\Delta^2 + \hbar^2 v_F^2 (k_x^2 + k_y^2 + k_z^2)}$ and $N_\pm$ is the norm of the states.

Surface states appear in this model if the gap parameter Δ changes its sign at the boundary, so that, for example, $\Delta > 0$ in the inside, and $\Delta < 0$ in the vacuum. The model also allows for the analytical computation of the surface bands of a cylinder,[13]

as shown in Appendix A. Later we also include quadratic corrections to the Hamiltonian in Eq. (1) and we show that boundary conditions need to be chosen appropriately in that case.

To obtain the solution of the Hamiltonian, Eq. (1), on a sphere, we rephrase its eigenvalue equations into spherical coordinates by matching. The eigenvector of energy E, $\Psi \equiv (\Psi_A, \Psi_B, \Psi_C, \Psi_D)$, satisfies the equations

$$\begin{aligned}
(E-\Delta)\Psi_A &= i\left[\cos(\theta)\partial_r - \frac{\sin(\theta)}{r}\partial_\theta\right]\Psi_B - ie^{-i\phi}\left[\sin(\theta)\partial_r + \frac{\cos(\theta)}{r}\partial_\theta - i\frac{1}{r\sin(\theta)}\partial_\phi\right]\Psi_D,\\
(E+\Delta)\Psi_B &= i\left[\cos(\theta)\partial_r - \frac{\sin(\theta)}{r}\partial_\theta\right]\Psi_A - ie^{-i\phi}\left[\sin(\theta)\partial_r + \frac{\cos(\theta)}{r}\partial_\theta - i\frac{1}{r\sin(\theta)}\partial_\phi\right]\Psi_C,\\
(E-\Delta)\Psi_C &= -ie^{i\phi}\left[\sin(\theta)\partial_r + \frac{\cos(\theta)}{r}\partial_\theta + i\frac{1}{r\sin(\theta)}\partial_\phi\right]\Psi_B - i\left[\cos(\theta)\partial_r - \frac{\sin(\theta)}{r}\partial_\theta\right]\Psi_D,\\
(E+\Delta)\Psi_D &= -ie^{i\phi}\left[\sin(\theta)\partial_r + \frac{\cos(\theta)}{r}\partial_\theta + i\frac{1}{r\sin(\theta)}\partial_\phi\right]\Psi_A - i\left[\cos(\theta)\partial_r - \frac{\sin(\theta)}{r}\partial_\theta\right]\Psi_C
\end{aligned} \tag{3}$$

(here $\hbar = v_F = 1$), with the boundary conditions

$$\Delta(r,\theta,\phi) = \begin{cases} \Delta_{\text{in}}, r < R, \\ \Delta_{\text{out}}, r > R. \end{cases} \tag{4}$$

We choose $\Delta_{\text{in}} = -\Delta_{\text{out}} = \Delta$ for simplicity, so that the exponential decay of the boundary states into the bulk near a flat surface is defined by the length scale $\Lambda = \hbar v_F/\Delta$. The angular momentum is conserved and is quantized in half-integer units (see, e.g., Ref. 16). Its eigenfunctions allow us to reduce the set of Eqs. (3) to two coupled differential equations for the radial coordinates, as discussed in Appendix B. It can be shown that the energy spectrum converges exponentially to the one for the $(2+1)$-dimensional Dirac equation on a sphere:

$$\begin{aligned}
E_J &= \pm\frac{\hbar v_F (J+1/2)}{R} \times [1 + \mathcal{O}(e^{-R/\Lambda})],\\
J &= \frac{1}{2}, \frac{3}{2}, \ldots, J_{\max},
\end{aligned} \tag{5}$$

where $J_{\max} \sim R/\Lambda$. The multiplicity of each level is $2J+1$. The exponential convergence of the energy levels to the asymptotic value in Eq. (5) is shown in Fig. 1. This type of convergence implies that the effective Hamiltonian describing the surface modes does not admit an expansion in higher order derivatives, of the type $\Delta(\Lambda\partial_i)^n$. The study of the Hamiltonian in Eq. (1) can be extended in a straightforward way to the case when $\Delta_{\text{out}} \neq \Delta_{\text{in}}$, although it becomes cumbersome to obtain analytical expansions in the limit $R \to \infty$. The numerical solution, obtained by generalizing the analysis in Appendix B, shows agreement with the spectrum in Eq. (5) of the same accuracy as those reported in Fig. 1.

As quadratic terms do not break the spherical symmetry, they can be safely added to Eq. (1), by the simple substitution $\Delta \to \Delta + \alpha(k_x^2 + k_y^2 + k_z^2)$, where α is a constant. Hence the angular part of the wave functions remains unchanged, while its radial part satisfies second-order coupled equations, in place of those in Eq. (3). For each value of the energy, E, we find evanescent waves with two different decay lengths, $\Lambda_1(E)$ and $\Lambda_2(E)$, which are given by the roots of a fourth-order polynomial. The boundary conditions need to be replaced. The simplest boundary condition compatible with the new second-order equations is $\Psi_A(R) = \Psi_B(R) = \Psi_C(R) = \Psi_D(R) = 0$.[14] By solving these boundary conditions numerically, we find, again, an agreement with Eq. (5) similar to that shown in Fig. 1. Results are shown in Fig. 2.

We conclude that the boundary states on a spherical TI satisfy the Dirac equation on the surface of the sphere. The spin connection, related to the intrinsic curvature of the metric, clearly emerges at the boundaries of a TI. Therefore, the boundary states satisfy the Dirac equation on the curved space-time $S^2 \times R$ (see Ref. 10),

$$\gamma^\mu(\partial_\mu + \Gamma_\mu)\Psi = 0. \tag{6}$$

Here $\gamma^\mu = e_a{}^\mu \gamma^a$ (with $\gamma^{a=0} = -i\sigma^z$, $\gamma^{a=1} = \sigma^y$, and $\gamma^{a=2} = -\sigma^x$) are the rotated Dirac matrices, satisfying the generalization of the flat algebra

$$\{\gamma^\mu, \gamma^\nu\} = 2g^{\mu\nu}. \tag{7}$$

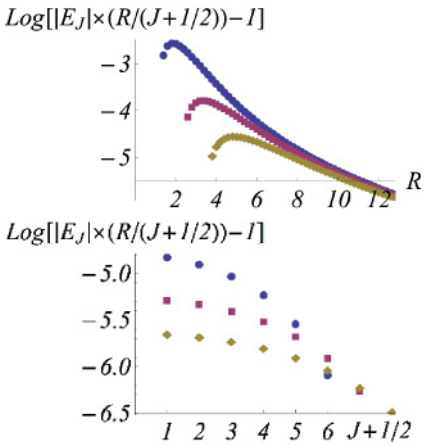

FIG. 1. (Color online) Dependence of the boundary energy levels on the angular momentum J and radius R. The deviation from the result for the $(2+1)$-dimensional Dirac equation on a sphere (see Eq. (5)]. Top: Dependence on R. From top to bottom, $J + 1/2 = 1,2,3$. Bottom: Dependence on J. From top to bottom, $R = 8,10,12$. In all cases, $v_F = 1$ and $\Delta = 1$.

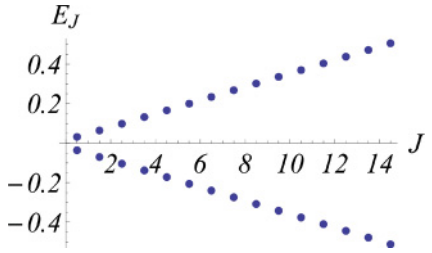

FIG. 2. (Color online) Energy levels of a spherical topological insulator of radius $R = 30$ with a quadratic dispersion relation, obtained by the replacement $\Delta \to \Delta + \alpha(k_x^2 + k_y^2 + k_z^2)$ in Eq. (1). Other parameters are $\Delta = 1$ and $v_F = 1$. Boundary conditions are $\Psi_A(R) = \Psi_B(R) = \Psi_C(R) = \Psi_D(R) = 0$.

The Minkowski metric η_{ab} has been replaced by the curved one,

$$g_{\mu\nu} = \mathrm{diag}(-1, R^2, R^2\cos^2\theta) = \eta_{ab}\, e^a{}_\mu e^b{}_\nu. \tag{8}$$

From this expression we can read off the tetrads. The term Γ_μ is the spin connection $\frac{i}{2}\Gamma^a{}_\mu{}^b\Sigma_{ab}$, where $\Sigma_{ab} = i/2[\gamma_a, \gamma_b]$ are the generators of the spinorial representation of the Lorentz group, and the connection coefficients $\Gamma^a{}_\mu{}^b$ are given by $\Gamma^a{}_\mu{}^b = e^a{}_\nu \nabla_\mu e^{b\nu}$. On using the tetrads implicitly defined in Eq. (8), it can be easily computed to be

$$\Gamma_\mu = -\frac{i}{2}\sigma_3 \sin\theta \delta_{2\mu}. \tag{9}$$

Therefore the Dirac equation, (6), can be solved (see, e.g., Ref. 17), yielding the eigenvalues E_J of Eq. (5). We show an application of this formalism in Sec. III.

III. SCATTERING OFF A GAUSSIAN BUMP

We now derive the resistivity for electrons propagating at the flat boundary surface of a TI, when they are scattered off a Gaussian bump of height $z(|\vec{r}|) = h\, e^{-r^2/\ell^2}$. The Boltzmann relaxation-time approximation can be used:

$$\rho(k_F) = \frac{2}{e^2 v_F^2 \nu(0)}\, \frac{1}{\tau(k_F)}, \tag{10}$$

where the usual definition of the total relaxation rate is

$$\frac{1}{\tau(k_F)} = \frac{2\pi}{\hbar}\nu(0)\int_0^{2\pi} d\theta (1 - \hat{k}\cdot\hat{k}')|\langle k|t^{\mathrm{eff}}|k'\rangle|^2, \tag{11}$$

and $\nu(0) = k_F/(\pi\hbar v_F)$ is the density of states at the Fermi level for both spins. Here $\langle k|t^{\mathrm{eff}}|k'\rangle$ is the matrix element of the t matrix, which depends on the energy and on the scattering angle θ between the incoming and the outgoing wave.

Since the metric induced on the manifold by the bump is axially symmetric, it is convenient to rewrite the $(2+1)$-dimensional Dirac equation in flat space time in cylindrical coordinates:

$$-i\hbar v_F\left(\sigma^r\partial_r + \sigma^\theta\,\frac{1}{r}\partial_\theta\right)\psi = E\psi, \tag{12}$$

where $\Psi(\vec{r},t) = e^{-iEt/\hbar}\psi(\vec{r})$ and the matrices $\sigma^{r,\theta}$ are $\sigma^r = \cos\theta\,\sigma^x + \sin\theta\,\sigma^y$ and $\sigma^\theta = -\sin\theta\,\sigma^x + \cos\theta\,\sigma^y$. Given the metric[18]

$$g_{\mu\nu} = \begin{pmatrix} -1 & 0 & 0 \\ 0 & 1+f(r) & 0 \\ 0 & 0 & r^2 \end{pmatrix}, \tag{13}$$

where $f(r) = [dz(r)/dr]^2$, we rewrite Eq. (6). As shown in Appendix C, the spin connection Γ_μ can be embodied in the wave function as a real prefactor $\psi = \Phi\exp\int_r^{+\infty} dr' A_\theta(r')$, where $A_\theta(r) = (\sqrt{1+f(r)} - 1)/2r$. The spinor Φ satisfies the equation

$$-i\left[\frac{\sigma^r}{\sqrt{1+f(r)}}\frac{\partial}{\partial r} + \sigma^\theta\frac{1}{r}\frac{\partial}{\partial\theta}\right]\Phi = sk\Phi, \tag{14}$$

where $s = +(-)$ for particles(holes), and $E = \hbar v_F k$. The real prefactor can be interpreted as the origin of charge puddles accumulating at the bump. Equation (14) describes an unrelaxed lattice. Relaxation of the structure, besides adding an effective gauge potential, may further change the spin connection. As elastic deformations do not add any curvature, the change only implies a trivial holonomy on the wave function. This is a way of restating the Saint Venant conditions for the two-dimensional case. Changes in the Dirac equations are well localized in space close to the bump, hence a scattering picture can be fruitfully adopted here. We focus on the particle sector of the theory and assume that the incoming k vector is in the direction of the polar axis ($\theta = 0$). The eigenfunctions can be expressed as a superposition of angular momentum m eigenstates:

$$\Phi_m(r,\theta) = \begin{pmatrix} u_m(r) \\ i\,v_m(r)e^{i\theta} \end{pmatrix} e^{im\theta}. \tag{15}$$

The Born approximation is worked out, to lowest order, in Appendix C. Using an asymptotic expansion of the wave functions given in Eq. (C9), we have

$$\frac{1}{\tau(\vec{k}_F)} = \frac{n_b v_F}{k_F} \times \sum_m [\sin^2\delta_m - \cos(\delta_{m+1} - \delta_{m-1})\sin\delta_{m+1}\sin\delta_{m+1}], \tag{16}$$

where the phase shifts δ_m for the mth component of the wave function are reported in Appendix C and n_b is the concentration of bumps.

At a low incoming electron energy, it turns out that the terms with $m = 0, \pm 1, \pm 2$ are $\mathcal{O}[(k\ell)^4]$, and when choosing $4\pi^2h^2/\ell^2 \sim 1$, they sum up to $\boldsymbol{\mathcal{S}} \approx 0.733$. The terms with $m = \pm 3$ are $\mathcal{O}[(k\ell)^8]$, while the terms $m = \pm 4$ are $\mathcal{O}[(k\ell)^{12}]$ (see Appendix C).

Eventually, the resistivity for independent point-like defects, when the carrier density is low (i.e., low incoming energy) is

$$\rho(k_F) \sim \frac{2h}{e^2}\, n_b \pi \ell^2 \left\{\mathcal{S}\left(\frac{h}{\ell}\right)(k_F\ell)^2 + \mathcal{O}[(k_F\ell)^4]\right\}. \tag{17}$$

$\boldsymbol{\mathcal{S}}(h/\ell)$ is a numerical prefactor that depends on the strength of the perturbation parametrized by h/ℓ. The plot of resistivity vs. energy in dimensionless units $k_F\ell$ for various values of h/ℓ

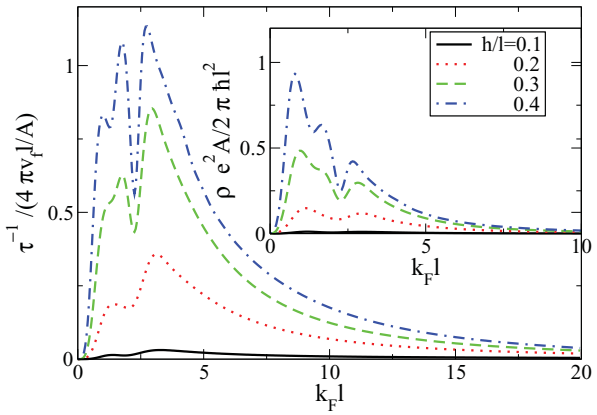

FIG. 3. (Color online) Inverse scattering time as a function of $k_F l$ for different values of the aspect ratio of the bump h/l. Inset: Resistivity due to scattering off a bump on the surface of a topological insulator, in units of $2\pi\hbar\ell^2/e^2A$, vs. dimensionless energy $k\ell$, at different ratios h/ℓ.

is shown in the inset in Fig. 3. The leading term is proportional to the density of carriers n. The conductivity $\sim\rho^{-1}$ grows linearly at large $k_F\ell$ and has a minimum in the neighborhood of $k_F\ell \sim 1$. In Fig. 3 the inverse relaxation time is reported vs. $k_F\ell$ in units of $A/4\pi v_F\ell$, where A is the surface area.

It has been proven recently that the classical limit for high incoming energy (i.e., relatively high densities n) corresponds to an energy-independent product, $v_F\tau(k_F)$.[9] This implies that, according to Eq. (10), $\rho \propto h/(e^2k_F) \sim 1/\sqrt{n}$, in this limit. We derive the same conclusion with a careful analysis of the sum in Eq. (16) at $k\ell \gg 1$. Classically, angular momentum conservation in the scattering implies that $m \sim kb$. Here b is the impact parameter measured from the center of the bump in the direction orthogonal to $\vec{k}$. By asymptotically expanding the Bessel functions appearing in the phase shifts, it turns out that there is a collection of terms contributing to the sum, which are roughly independent of m, as long as $k\ell \gg m$. For these m values, $\tan\delta_m$ is of the form

$$\tan\delta_m \approx \pi\left(\frac{h}{\ell}\right)^2 \frac{k\ell}{2}\left[\sqrt{\frac{\pi}{2}} - (-1)^m \frac{2}{(k\ell)^3}\right]. \qquad (18)$$

All other terms scale for $m \gg k\ell$ as

$$\sqrt{\frac{m}{2}}\left(\frac{k\ell}{2}\right)^{2(m+1)} \frac{1}{(2m-1)!!}, \qquad (19)$$

and therefore they rapidly converge to 0. We conclude that in the semiclassical limit $k\ell \gg 1$, a factor k_F comes from the relevant terms in the sum of Eq. (16), which are all of the same order. This factor cancels with the k_F appearing in the denominator, so that the result for $v_F\tau(k_F)$ is independent of k_F. This is, in fact, found numerically. In Appendix D we report a simple argument based on a saddle-point approximation of the $\sum_m$ that qualitatively recovers the classical limiting result for large $k_F\ell$. A significant increase in the cross section of the bump appears in Fig. 3 for $k_F\ell \sim 1$ and $h/\ell \gtrsim 0.2$. This increase is due to quantum resonances induced by the nontrivial spin connection.

IV. DISCUSSION

We have shown in Sec. II how the $(2+1)$-dimensional Dirac equation in curved two-dimensional space emerges at the simplest boundary with a nontrivial metric, the surface of a sphere. The metric enters through the spin connection, which reflects the properties of the internal spin under parallel transport along the surface.[10] The spin connection reflects a quantum feature of the electrons and cannot be inferred from solely classical arguments. The spin connection leads to a finite Berry phase when the electron is transported around a closed geodesic. A manifestation of this effect is the quantization of the total angular momentum in half-integer units.

The linearized model that we have studied leads to simple analytical expressions of the energies and wave functions of the boundary states. They can be used as a zeroth approximation to situations close to spherical symmetry or where an isotropic electronic structure can be obtained by rescaling a length. We find that the corrections to the $(2+1)$-dimensional Dirac equation depend exponentially on $R/\Lambda \equiv R\Delta/\hbar v_F$.[19]

The model describes external surfaces of mesoscopic crystals and internal voids in bulk systems. In the case of a small void, we find that two doublets at a finite distance of the Dirac energy appear for radii $R \gtrsim 2/\Lambda$. These voids will act as molecules embedded into the bulk material. The interaction energy of electrons localized inside the voids scales as the level separation, $E_{\rm int} \approx e^2/(\epsilon R)$, where ϵ is the dielectric constant of the topological insulator. At temperatures below this scale, voids with an odd number of electrons will give rise to magnetic moments. The RKKY interaction between moments at different vacancies should decay exponentially, $J_{\rm RKKY}(\vec{\mathbf{r}} - \vec{\mathbf{r}}') \sim e^{-|\vec{\mathbf{r}}-\vec{\mathbf{r}}'|/\Lambda}$. Hence, small vacancies might give rise to a paramagnetic susceptibility in topological insulators. If they are within a distance $d \sim \Lambda$ from the surface, these local moments will hybridize with the surface states, leading to the Kondo effect.[20,21]

We have analyzed the scattering of Dirac fermions by surface corrugations that induce a nontrivial curvature in the quantum limit, $k_F\ell \lesssim 1$. We find that the resistivity due to a finite concentration of bumps, n_b, vanishes as k_F^2 for small k_F, due to a combination of a density of states factor, which goes as k_F, and a scattering time that increases as k_F^{-3}. By comparison, the scattering time in the classical regime[9] ($k_F\ell \to \infty$) is independent of k_F, and $\rho \sim k_F^{-1}$. The wave nature of the quasiparticles allows them to diffract around the bump, making it effectively transparent for long wavelengths, $k_F\ell \ll 1$. The nontrivial curvature induces quantum resonances for $k_F\ell \sim 1$ and an aspect ratio $h/\ell \gtrsim 0.2$.

ACKNOWLEDGMENTS

We acknowledge important discussions with A. Akhmerov, R. Egger, and M. A. H. Vozmediano. P.L. acknowledges financial support from FP7/2007-2013 under the grants MIDAS (Macroscopic Interference Devices for Atomic and Sold State Physics) and N. 264098 - MAMA (Multifunctioned Advanced Materials and Nanoscale Phenomena). F.G. is supported by MICINN (Spain) Grant No. FIS2008-00124 and CONSOLIDER Grant No. CSD2007-00010.

APPENDIX A: BOUNDARY STATES AT THE CYLINDER SURFACE

In the appendixes we use $\hbar = v_F = 1$, except for the main results. Let us start from the $\vec{k}\cdot\vec{p}$ model Hamiltonian of Eq. (1):

$$H[\vec{r}] = \begin{pmatrix} \Delta & i\partial_z & 0 & i(\partial_x + i\partial_y) \\ i\partial_z & -\Delta & i(\partial_x + i\partial_y) & 0 \\ 0 & i(\partial_x - i\partial_y) & \Delta & -i\partial_z \\ i(\partial_x - i\partial_y) & 0 & -i\partial_z & -\Delta \end{pmatrix}. \tag{A1}$$

To find surface states in this approximation, it is enough to match the solutions of the Schrödinger equation at the surface of the cylinder. The gap Δ should change its sign between in and out of the surface. We rewrite the eigenvalue problem in cylindrical coordinates for the four-component spinor $(\Psi_A, \Psi_B, \Psi_C, \Psi_D)$:

$$\begin{aligned}
(E-\Delta)\Psi_A(\vec{\mathbf{r}}) &= i\frac{\partial}{\partial_z}\Psi_B(\vec{\mathbf{r}}) + e^{i\theta}\left(i\frac{\partial}{\partial r} - \frac{1}{r}\frac{\partial}{\partial\theta}\right)\Psi_D(\vec{\mathbf{r}}), \\
(E+\Delta)\Psi_B(\vec{\mathbf{r}}) &= i\frac{\partial}{\partial_z}\Psi_A(\vec{\mathbf{r}}) + e^{i\theta}\left(i\frac{\partial}{\partial r} - \frac{1}{r}\frac{\partial}{\partial\theta}\right)\Psi_C(\vec{\mathbf{r}}), \\
(E-\Delta)\Psi_C(\vec{\mathbf{r}}) &= e^{-i\theta}\left(i\frac{\partial}{\partial r} + \frac{1}{r}\frac{\partial}{\partial\theta}\right)\Psi_B(\vec{\mathbf{r}}) - i\frac{\partial}{\partial_z}\Psi_D(\vec{\mathbf{r}}), \\
(E+\Delta)\Psi_D(\vec{\mathbf{r}}) &= e^{-i\theta}\left(i\frac{\partial}{\partial r} + \frac{1}{r}\frac{\partial}{\partial\theta}\right)\Psi_A(\vec{\mathbf{r}}) - i\frac{\partial}{\partial_z}\Psi_C(\vec{\mathbf{r}})
\end{aligned} \tag{A2}$$

(in the following k is in the $\hat{z}$ direction, which is the axis of the infinite cylinder of radius R). Inside the cylinder, the wave functions, which are mostly localized close to the surface, involve the modified Bessel functions $I_n(\kappa r)$ with integer n. They diverge exponentially at infinity but are finite for $r \to 0$. The two eigenfunctions at fixed energy E are (κ is to be determined by self-consistency in the following)

$$|E,1_<\rangle = \frac{1}{N}\begin{pmatrix} (E+\Delta)I_n(\kappa r) \\ k\, I_n(\kappa r) \\ 0 \\ i\kappa I_{n+1}(\kappa r)e^{-i\theta} \end{pmatrix} e^{-in\theta}e^{-ikz}, \quad |E,2_<\rangle = \frac{1}{N}\begin{pmatrix} i\kappa I_n(\kappa r)e^{i\theta} \\ 0 \\ -kI_{n+1}(\kappa r) \\ (E-\Delta)I_{n+1}(\kappa r) \end{pmatrix} e^{-i(n+1)\theta}e^{-ikz}. \tag{A3}$$

The energies of these states are $E = \pm\sqrt{\Delta^2 + k^2 - \kappa^2}$. Outside the cylinder, the functions $K_n(\kappa r)$ replace the $I_n(\kappa r)$, as the former decay exponentially for $\kappa r \to \infty$ and $\Delta \to -\Delta$. The eigenfunctions are

$$|E,1_>\rangle = \frac{1}{N}\begin{pmatrix} (E-\Delta)K_n(\kappa r) \\ kK_n(\kappa r) \\ 0 \\ -i\kappa K_{n+1}(\kappa r)e^{-i\theta} \end{pmatrix} e^{-in\theta}e^{-ikz}, \quad |E,2_>\rangle = \frac{1}{N}\begin{pmatrix} -i\kappa K_n(\kappa r)e^{i\theta} \\ 0 \\ -kK_{n+1}(\kappa r) \\ (E+\Delta)K_{n+1}(\kappa r) \end{pmatrix} e^{-i(n+1)\theta}e^{-ikz}. \tag{A4}$$

The eigenvalues are the same as for Eq. (A3).

The two wave functions inside the cylinder should be matched to the two outside for each value of n. The matching conditions at R lead to

$$\mathrm{Det}\begin{vmatrix} i\kappa I_n(\kappa R) & (E+\Delta)I_n(\kappa R) & -i\kappa K_n(\kappa R) & (E-\Delta)K_n(\kappa R) \\ 0 & kI_n(\kappa R) & 0 & kK_n(\kappa R) \\ -kI_{n+1}(\kappa R) & 0 & -kK_{n+1}(\kappa R) & 0 \\ (E-\Delta)I_{n+1}(\kappa R) & i\kappa I_{n+1}(\kappa R) & (E+\Delta)K_{n+1}(\kappa R) & -i\kappa K_{n+1}(\kappa R) \end{vmatrix} = 0. \tag{A5}$$

The vanishing of the determinant implies

$$\left[I_n^2\, K_{n+1}^2 + K_n^2 I_{n+1}^2\right]\kappa^2 + (2\kappa^2 - 4\Delta^2)I_n I_{n+1} K_n K_{n+1} = 0. \tag{A6}$$

The presence of products of the Bessel functions I_n and K_n assures that, in the limit of $\kappa R \gg 1$, there is just an inverse power law dependence of the secular problem on κR. Equation (A6) becomes

$$\kappa^2 = \Delta^2\left[1 - \frac{(n+1/2)^2}{\Delta^2 R^2}\right]. \tag{A7}$$

Hence, according to Eq. (A8), the energy of the states is

$$E = \pm\hbar v_F\sqrt{k^2 + \frac{(n+1/2)^2}{R^2}} + \mathcal{O}\left(\frac{\hbar v_F^2}{\Delta^2 R^2}\right), \quad R \gg \frac{\hbar v_F}{\Delta}. \tag{A8}$$

This result is in complete agreement with Eq. (7) of Ref. 22 and Eq. (5) of Ref. 13. Let us now consider the opposite limit, $\kappa R \ll 1$. Expansion gives, up to second order in $1/\kappa R$,

$$\kappa^2 \left\{ 2n(n+1)\left[1+\frac{1}{16\,n^2(n+1)^2}\right]+\frac{1}{2}\right\} = \Delta^2. \tag{A9}$$

The energy reads, in this limit,

$$E_n(k) \approx \pm\Delta\sqrt{1-1\Big/\left(2n(n+1)\left[1+\frac{1}{16\,n^2(n+1)^2}\right]+\frac{1}{2}\right)+\left(\frac{\hbar v_F k_z}{\Delta}\right)^2}+\mathcal{O}\left(\frac{\hbar\Delta R}{v_F}\right) \quad \text{for} \quad R \ll \hbar v_F/\Delta. \tag{A10}$$

The given spectrum could be easily recovered using the tetrad formalism and by noting that there is no intrinsic curvature or spin connection on the surface of the cylinder.[22]

APPENDIX B: EIGENSTATES AND EIGENENERGIES ON THE BOUNDARY OF A SPHERE

Generalized angular momentum operators J can be defined as usual as the sum of spin and orbital angular momentum. It can be shown that the Hamiltonian in Eq. (3) commutes with J^2, J_z; therefore, its eigenstates can be labeled $|j,m\rangle$, with $\vec{\mathbf{J}}^2|j,m\rangle = j(j+1)|J,J_z\rangle$ and $J_z|j,m\rangle = m|J,J_z\rangle$. To obtain single-valued eigenfunctions, the values of J and J_z must be half-integers. As usual, by using $J^+|j;j\rangle = 0$ and $J^-|j,m\rangle \propto |j,m-1\rangle$, we can explicitly construct the wave functions of the different states $|j,m\rangle$. The Hamiltonian eigenfunction can thus be expanded onto the lowest angular momentum states:

$$\begin{aligned}
\left|\frac{1}{2},\frac{1}{2}\right\rangle &= A\begin{pmatrix}-\cos(\theta)\\0\\\sin(\theta)e^{i\phi}\\0\end{pmatrix}+B\begin{pmatrix}0\\-\cos(\theta)\\0\\\sin(\theta)e^{i\phi}\end{pmatrix}+C\begin{pmatrix}1\\0\\0\\0\end{pmatrix}+D\begin{pmatrix}0\\1\\0\\0\end{pmatrix},\\
\left|\frac{1}{2},-\frac{1}{2}\right\rangle &= A\begin{pmatrix}\sin(\theta)e^{-i\phi}\\0\\\cos(\phi)\\0\end{pmatrix}+B\begin{pmatrix}0\\\sin(\theta)e^{-i\phi}\\0\\\cos(\phi)\end{pmatrix}+C\begin{pmatrix}0\\0\\1\\0\end{pmatrix}+D\begin{pmatrix}0\\0\\0\\1\end{pmatrix},\\
\left|\frac{3}{2},\frac{3}{2}\right\rangle &= A\begin{pmatrix}-\sin(\theta)\cos(\theta)e^{i\phi}\\0\\\sin^2(\theta)e^{2i\phi}\\0\end{pmatrix}+B\begin{pmatrix}0\\-\sin(\theta)\cos(\theta)e^{i\phi}\\0\\\sin^2(\theta)e^{2i\phi}\end{pmatrix}+C\begin{pmatrix}\sin(\theta)e^{i\phi}\\0\\0\\0\end{pmatrix}+D\begin{pmatrix}0\\\sin(\theta)e^{i\phi}\\0\\0\end{pmatrix},\\
\left|\frac{3}{2},\frac{1}{2}\right\rangle &= A\begin{pmatrix}-2\cos^2(\theta)+\sin^2(\theta)\\0\\3\sin(\theta)\cos(\theta)e^{i\phi}\\0\end{pmatrix}+B\begin{pmatrix}0\\-2\cos^2(\theta)+\sin^2(\theta)\\0\\3\sin(\theta)\cos(\theta)e^{i\phi}\end{pmatrix}+C\begin{pmatrix}2\cos(\theta)\\0\\\sin(\theta)e^{i\phi}\\0\end{pmatrix}+D\begin{pmatrix}0\\2\cos(\theta)\\0\\\sin(\theta)e^{i\phi}\end{pmatrix},
\end{aligned} \tag{B1}$$

where the states $|3/2,-1/2\rangle, |3/2,-3/2\rangle$ are not explicitly exhibited here. Boundary states in the spherical case for $j = m = n-1/2$ $(n>0)$ have the following form:

$$\left\langle r,\theta,\phi\left|J-\frac{1}{2},J_z-\frac{1}{2}\right.\right\rangle = f_1^{\mp}(r)\begin{pmatrix}0\\-\cos\theta\sin^{n-1}\theta e^{i(n-1)\phi}\\0\\\sin^n\theta e^{in\phi}\end{pmatrix}+f_2^{\mp}(r)\begin{pmatrix}\sin^{n-1}\theta e^{i(n-1)\phi}\\0\\0\\0\end{pmatrix}. \tag{B2}$$

Here $f^-(r)$ and $f^+(r)$ are radial functions localized at the boundary for $r<R$ and $r>R$, respectively, and they satisfy the equations

$$\begin{aligned}
(E\mp\Delta)f_2^{\mp} &= -i\partial_r f_1^{\mp}-\frac{i}{r}(n+1)f_1^{\mp},\\
(E\pm\Delta)f_1^{\mp} &= -i\partial_r f_2^{\mp}+\frac{i}{r}(n-1)f_2^{\mp}.
\end{aligned} \tag{B3}$$

The system can be decoupled in a pair of Bessel equations:

$$\begin{aligned}\frac{d^2}{dr^2}f_1^{\pm}+\frac{2}{r}\frac{d}{dr}f_1^{\pm}-\left[(\Delta^2-E^2)+\frac{n(n+1)}{r^2}\right]f_1^{\pm}=0,\\ \frac{d^2}{dr^2}f_2^{\pm}+\frac{2}{r}\frac{d}{dr}f_2^{\pm}-\left[(\Delta^2-E^2)+\frac{n(n-1)}{r^2}\right]f_2^{\pm}=0,\end{aligned} \tag{B4}$$

whose solutions are

$$\begin{aligned}&\text{if}\quad r<R \qquad \begin{cases}f_1^-(r)=-i\frac{\Delta-E}{\kappa}C^-i_n(\kappa r),\\ f_2^-(r)=C^-i_{n-1}(\kappa r);\end{cases}\\ &\text{if}\quad r>R \qquad \begin{cases}f_1^+(r)=-iC^+\frac{\Delta+E}{\kappa}k_n(\kappa r),\\ f_2^+(r)=C^+k_{n-1}(\kappa r);\end{cases}\end{aligned} \tag{B5}$$

where i_n,k_n are the modified spherical Bessel functions:

$$i_n(x)\equiv\sqrt{\frac{\pi}{2x}}I_{n+\frac{1}{2}}(x),\quad k_n(x)\equiv\sqrt{\frac{\pi}{2x}}K_{n+\frac{1}{2}}(x). \tag{B6}$$

The matching conditions can be written using Eq. (B5):

$$\begin{cases}-iC^-(\Delta-E)i_n(\kappa R)=-iC^+(\Delta+E)k_n(\kappa R),\\ C^-i_{n-1}(\kappa R)=C^+k_{n-1}(\kappa R),\end{cases} \tag{B7}$$

which give rise to an implicit equation for the eigenenergies of the system:

$$\frac{\Delta-E}{\Delta+E}=-\frac{k_n(\kappa R)i_{n-1}(\kappa R)}{i_n(\kappa R)k_{n-1}(\kappa R)}. \tag{B8}$$

In the limit $\Delta R\to\infty$, this equation gives the admissible values of the energy,

$$E_n=\pm n\frac{\hbar v_F}{R},\quad n=1,\ldots,n_{\max}, \tag{B9}$$

consistent with Eq. (5).

APPENDIX C: DERIVATION OF THE ELASTIC *t* MATRIX FOR SCATTERING OFF A GAUSSIAN BUMP

We derive the elastic t matrix when a localized deformation is present on the surface of a TI. As in Ref. 18 we consider a two-dimensional spatial sheet modeled on a two-dimensional axially symmetric manifold with a single Gaussian bump. The axially symmetric Gaussian surface may be represented in Minkowski space time by the function $\phi=[t,x,y,h(r)]$, with $r^2=x^2+y^2$. From Eqs. (13), we may read the tetrads

$$\begin{aligned}e_x{}^1=\frac{\cos\theta}{\sqrt{1+f(r)}},\quad e_y{}^1=\frac{\sin\theta}{\sqrt{1+f(r)}},\\ e_x{}^2=-\frac{\sin\theta}{r},\quad e_y{}^2=\frac{\cos\theta}{r}.\end{aligned} \tag{C1}$$

The Dirac equation on a radially symmetric manifold is

$$-i\left[\frac{\sigma^r}{\sqrt{1+f(r)}}\partial_r+\sigma^\theta\left(\frac{1}{r}\partial_\theta+\frac{i}{2r}\left(1-\frac{1}{\sqrt{1+f(r)}}\right)\sigma^z\right)\right]\Psi=E\Psi. \tag{C2}$$

The gauge potential in Eq. (C2) is the spin connection,

$$\Gamma_\mu=\frac{i}{2}\left(1-\frac{1}{\sqrt{1+f(r)}}\right)\sigma^z\delta_{\mu 2}. \tag{C3}$$

Γ_μ can be gauged away, redefining the wave function with a real prefactor $\Psi\to\Phi\exp\int_r^{+\infty}dr'A_\theta(r')$, where $A_\theta=(\sqrt{1+f(r)}-1)/2r$. The m component of the spinor Φ has the form (m is the angular momentum integer)

$$\Phi_m(r,\theta|\vec{k},s)=\begin{pmatrix}u_{sm}(r)\\ \text{is}\quad v_{sm}(r)\,e^{i\theta}\end{pmatrix}e^{im(\theta-\theta_k)}, \tag{C4}$$

where θ_k is the angle that the direction of the $\vec{k}$ vector of the incoming wave forms with the polar axis. Substituting (C4) into the Dirac Eq. (14) and dropping the labels sm, we find that the functions $u(r), v(r)$ have to satisfy the following equations:

$$\begin{aligned}
&\frac{1}{\sqrt{1+f}}\frac{d^2u(r)}{dr^2}+\frac{1}{r}\frac{du(r)}{dr}+\left(\frac{d}{dr}\frac{1}{\sqrt{1+f}}\right)\frac{du(r)}{dr}-\frac{m^2}{r^2}\sqrt{1+f}\,u(r)+k^2u(r)=0,\\
&\frac{1}{\sqrt{1+f}}\frac{d^2v(r)}{dr^2}+\frac{1}{r}\frac{dv(r)}{dr}+\left(\frac{d}{dr}\frac{1}{\sqrt{1+f}}\right)\frac{dv(r)}{dr}-\frac{(m+1)^2}{r^2}\sqrt{1+f}\,v(r)+k^2v(r)=0.
\end{aligned} \tag{C5}$$

Due to the symmetry of the problem it is suitable to expand the Green's function for the flat space-time problem in polar coordinates,

$$G(z,z')=\frac{1}{2\pi}\sum_{m=-\infty}^{+\infty}e^{im(\theta-\theta')}g_m(r,r'). \tag{C6}$$

The Green's function displaying the correct jump of the derivative at $r=r'$ is

$$g_m(x,x')=2\pi^2 J_m(x_<)\,Y_m(x_>). \tag{C7}$$

Here $r_<(r_>)$ is the smaller(larger) of the two arguments r,r'. We now specialize the shape of the bump $h(r)$ to be the Gaussian bump $z(|\vec{r}|)$ defined in Sec. III A. This implies that $f(r)=(4h^2r^2/\ell^4)e^{-2(r/\ell)^2}$. We assume that the ratio h/ℓ is low, so that we can expand Eqs. (C5) by retaining just the lowest power of h/ℓ. By comparison with the system for the flat space [i.e., $f(r)=0$], we define the perturbative potential

$$\frac{h^2}{\ell^2}V_m(r)=\frac{2h^2}{\ell^4}r^2e^{-2r^2/\ell^2}\left[\frac{d^2}{dr^2}+\left(\frac{4}{r}-\frac{8r}{\ell^2}\right)\frac{d}{dr}-\frac{m^2}{r^2}\right]. \tag{C8}$$

In the Born approximation, the Dyson equation for, for example, u_{km} reads

$$\begin{aligned}
u_{km}(r)&=J_m(kr)+\frac{h^2}{\ell^2}\int_0^\infty dr'r'g_m(r,r')V_m(r')J_m(kr')\\
&=J_m(kr)+\frac{2h^2}{\ell^4}\int_0^\infty dr'g_m(r,r')r'^3e^{-2r'^2/\ell^2}\left\{k^2+\left(\frac{3}{r'}-\frac{8r'}{\ell^2}\right)\frac{d}{dr'}\right\}J_m(kr')
\end{aligned} \tag{C9}$$

We have used the fact that J_m solves the Bessel differential equation to simplify the action of V_m on J_m itself. By defining

$$\tan\delta_m=\frac{4\pi^2k^2h^2}{\ell^4}\int_0^\infty dr'J_m(kr')r'^3e^{-2r'^2/\ell^2}\left\{1+\frac{1}{k^2}\left(\frac{3}{r'}-\frac{8r'}{\ell^2}\right)\frac{d}{dr'}\right\}J_m(kr'), \tag{C10}$$

the scattering state for $r/\ell\to\infty$ takes the form $u_{km}(r)\sim J_m(kr)+\tan\delta_m\,Y_m(kr)$.

The integrals in Eq. (C10) can be evaluated analytically. The asymptotic expansion of the Bessel functions implies that, far from the bump($r/\ell\to\infty$), the outgoing wave takes the form

$$u_{km}(r)\sim_{r/\ell\to\infty}\frac{1}{\sqrt{1+\tan^2\delta_m}}\cos\chi_m+\frac{\tan\delta_m}{\sqrt{1+\tan^2\delta_m}}\sin\chi_m\equiv\cos(\chi_m+\delta_m),\quad \chi_m=kr-\frac{m\pi}{2}-\frac{\pi}{4}.$$

Our result is valid for both components of the spinor solution given by Eq. (15). On exploiting the symmetry of the Dirac massless equation with respect to replacements $u\leftrightarrow v$, $m\leftrightarrow -m-1$, it is easy to see that the sums that include δ_m, for all m, are equal.

We now evaluate the t-matrix element for a scattering event, in which an incoming wave with wave vector $\vec{k}$ is scattered elastically by the Gaussian bump and a plane wave of wave vector $\vec{p}$ emerges. The t-matrix element is

$$\langle p|t(\vec{k})|k\rangle=[1+e^{-i(\theta_p-\theta_k)}]\sqrt{\frac{2}{\pi kR^2}}e^{i\pi/4}\frac{1}{R}\int_0^R dr\,e^{\frac{h^2}{\ell^4}\int_r^R dr'r'^2e^{-2(r'/\ell)^2}}\sum_m[e^{2i\delta_m}-1]\,e^{-im(\theta_p-\theta_k)}.$$

The space integral arises from the exponential prefactor of Ψ defined before Eq. (14). To evaluate the relaxation time formula of Eq. (16), we first perform the integral over the angle θ_p of the square modulus of the angle-dependent exponentials in the sums. The integral is nonvanishing only for $m-m'=\pm2,0$. By rearranging the sums, then Eq. (16) is obtained.

APPENDIX D: SEMICLASSICAL APPROXIMATION FOR THE INVERSE RELATION TIME

In this section we present a tasteful derivation of the classical high-energy limit for the relaxation time. The latter can be obtained by assuming classical diffusion along the geodesic trajectories across the bump and yields[9]

$$\frac{1}{\tau} \approx \frac{v_F}{2A} \int db\, \theta^2(b). \tag{D1}$$

Here b is the impact parameter of the incoming particle, while θ is the scattering angle and A is the area of the sample. The starting point is the usual expression for the relaxation time of Eq. (16):

$$\frac{1}{\tau} = \frac{v_F}{kA} \int_0^{\pi} d\theta (1-\cos\theta) \left| \sum_m f_m(\theta) \right|^2, \tag{D2}$$

given in terms of the scattering amplitudes $f_m(\theta) = [e^{i2\delta_m} - 1]e^{im\theta}$. At high energy, many m terms contribute to the sum, so that we take its continuum limit, which amounts to integrating over continuous values of the classical angular momentum $m = kb$. As forward scattering is excluded form Eq. (D2), it is enough to apply the saddle-point approximation to the resulting integral:[23]

$$\sum_m e^{i(2\delta_m + m\theta)} \approx e^{i(2\delta_{m_0} + m_0\theta)} \times \int dm\, e^{i\frac{d^2\delta}{dm^2}|_0 (m-m_0)^2}. \tag{D3}$$

Here m_0 is the stationary point, which solves the saddle-point equation:

$$\left. \frac{d\delta_m}{dm} \right|_{m_0} - \frac{\theta}{2} = 0. \tag{D4}$$

Derivation of this equation, once more, provides a relation between the second derivative of the phase shift δ_m and the angle θ

$$\frac{d^2\delta_m}{dm^2} - \frac{1}{2}\frac{d\theta}{dm} = 0. \tag{D5}$$

An analytical continuation in the complex m plane allows us to make the integral converge. Gaussian integration in Eq. (D3) implies that

$$\left| \sum_m f_m(\theta) \right|^2 \approx \pi \left| \frac{dm}{d\theta} \right|, \tag{D6}$$

thus yielding the expected result:

$$\begin{aligned} \frac{1}{\tau} &\sim \frac{v_F}{k}\frac{1}{A} \int d\theta (1-\cos\theta) \left| \frac{dm}{d\theta} \right| \\ &\sim \frac{v_F}{k}\frac{1}{A} \int dm \frac{\theta^2}{2} \sim \frac{v_F}{A} \int db \theta^2(b). \end{aligned} \tag{D7}$$

In the last equality the conservation of the angular momentum $m = kb$ has been exploited, together with the remark that the scattering angle depends only on b in the classical diffusion. This reproduces the desired high-energy behavior.

The analysis of Eq. (16) provides a similar conclusion. The quantity $\delta_{m+1} - \delta_{m-1}$, appearing as the argument of the cosine, is $\approx 2d\delta_m/dm$. At high incoming energies, $\delta_m \approx (2m+1)\pi/2$, which is consistent with the asymptotic form of the wave function given in Eq. (C11). To lowest order we get, according to Eq. (D4),

$$\sin^2\delta_m - \cos(\delta_{m+1} - \delta_{m-1}) \sin\delta_{m+1} \sin\delta_{m-1} \approx \frac{\theta^2}{2}, \tag{D8}$$

so that we again recover

$$\frac{1}{\tau} \approx \frac{v_F}{kA} \int dm \frac{\theta^2}{2} \approx \frac{v_F}{A} \int db\, \theta(b)^2. \tag{D9}$$

---

*Corresponding author: parente@na.infn.it

[1] L. Fu, C. L. Kane, and E. J. Mele, Phys. Rev. Lett. **98**, 106803 (2007).

[2] L. Fu and C. L. Kane, Phys. Rev. B **76**, 045302 (2007).

[3] J. E. Moore and L. Balents, Phys. Rev. B **75**, 121306(R) (2007).

[4] M. Z. Hasan and C. L. Kane, Rev. Mod. Phys. **82**, 3045 (2010).

[5] Y. Ran, Y. Zhang, and A. Vishwanath, Nature Phys. **5**, 298 (2009).

[6] J. C. Y. Teo and C. L. Kane, Phys. Rev. Lett. **104**, 046401 (2010).

[7] J. C. Y. Teo and C. L. Kane, Phys. Rev. B **82**, 115120 (2010).

[8] A. H. Castro Neto, F. Guinea, N. M. R. Peres, K. S. Novoselov, and A. K. Geim, Rev. Mod. Phys. **81**, 109 (2009).

[9] J. P. Dahlhaus, C.-Y. Hou, A. R. Akhmerov, and C. W. J. Beenakker, Phys. Rev. B **82**, 085312 (2010).

[10] M. Nakahara, *Geometry, Topology and Physics* (Adam Hilger, London, 1990).

[11] D.-H. Lee, Phys. Rev. Lett. **103**, 196804 (2009).

[12] A. Cortijo and M. A. H. Vozmediano, Nucl. Phys. B **763**, 293 (2007).

[13] R. Egger, A. Zazunov, and A. L. Yeyati, Phys. Rev. Lett. **105**, 136403 (2010).

[14] W.-Y. Shan, H.-Z. Lu, and S.-Q. Shen, New J. Phys. **12**, 043048 (2010).

[15] H. Zhang, C.-X. Liu, X.-L. Qi, X. Dai, Z. Fang, and S.-C. Zhang, Nature Phys. **5**, 438 (2009).

[16] J. González, F. Guinea, and M. A. H. Vozmediano, Phys. Rev. Lett. **69**, 172 (1992).

[17] G. Miele and P. Vitale, Nucl. Phys. B **494**, 365 (1997).

[18] F. de Juan, A. Cortijo, and M. A. H. Vozmediano, Phys. Rev. B **76**, 165409 (2007).

[19] The carbon fullerenes admit a continuum description in terms of two Dirac equations on the surface of a sphere.[16] Lattice effects, such as scattering between the two equations, lead to corrections that scale as $(a/R)^2$, where a is the lattice spacing (see Ref. 24). We do not find terms of a similar magnitude at the surface of a topological insulator.

[20]X.-Y. Feng, W.-Q. Chen, J.-H. Gao, Q.-H. Wang, and F.-C. Zhang, Phys. Rev. B **81**, 235411 (2010).
[21]R. Žitko, Phys. Rev. B **81**, 241414 (2010).
[22]Y. Zhang, Y. Ran, and A. Vishwanath, Phys. Rev. B **79**, 245331 (2009).
[23]L. Landau and L. Lifshitz, *Quantum Mechanics Non-Relativistic Theory* (Butterworth-Heinemann, London, 1981).
[24]F. Guinea, J. González, and M. A. H. Vozmediano, Phys. Rev. B **47**, 16576 (1993).